WATER RESEARCH 45 (2011) 2573–2586

Available at www.sciencedirect.com

ScienceDirect

journal homepage: www.elsevier.com/locate/watres

Assessment of global nitrogen pollution in rivers using an integrated biogeochemical modeling framework

Bin He [a,b,*], Shinjiro Kanae [c], Taikan Oki [d], Yukiko Hirabayashi [e], Yosuke Yamashiki [b], Kaoru Takara [b]

[a] Center for Promotion of Interdisciplinary Education and Research, Educational Unit for Adaptation and Resilience for a Sustainable Society, Kyoto University, Kyoto, Japan
[b] Disaster Prevention Research Institute (DPRI), Kyoto University, Kyoto, Japan
[c] Department of Mechanical and Environmental Informatics, Tokyo Institute of Technology, Japan
[d] Institute of Industrial Science, The University of Tokyo, Japan
[e] Institute of Engineering Innovation, The University of Tokyo, Japan

ARTICLE INFO

Article history:
Received 14 September 2010
Received in revised form
3 February 2011
Accepted 10 February 2011
Available online 19 February 2011

Keywords:
Global rivers
Water quality
Nitrogen pollution load
Terrestrial ecosystem
Anthropogenic sources

ABSTRACT

This study has analyzed the global nitrogen loading of rivers resulting from atmospheric deposition, direct discharge, and nitrogenous compounds generated by residential, industrial, and agricultural sources. Fertilizer use, population distribution, land cover, and social census data were used in this study. A terrestrial nitrogen cycle model with a 24-h time step and 0.5° spatial resolution was developed to estimate nitrogen leaching from soil layers in farmlands, grasslands, and natural lands. The N-cycle in this model includes the major processes of nitrogen fixation, nitrification, denitrification, immobilization, mineralization, leaching, and nitrogen absorption by vegetation. The previously developed Total Runoff Integrating Pathways network was used to analyze nitrogen transport from natural and anthropogenic sources through river channels, as well as the collecting and routing of nitrogen to river mouths by runoff. Model performance was evaluated through nutrient data measured at 61 locations in several major world river basins. The dissolved inorganic nitrogen concentrations calculated by the model agreed well with the observed data and demonstrate the reliability of the proposed model. The results indicate that nitrogen loading in most global rivers is proportional to the size of the river basin. Reduced nitrate leaching was predicted for basins with low population density, such as those at high latitudes or in arid regions. Nitrate concentration becomes especially high in tropical humid river basins, densely populated basins, and basins with extensive agricultural activity. On a global scale, agriculture has a significant impact on the distribution of nitrogenous compound pollution. The map of nitrate distribution indicates that serious nitrogen pollution (nitrate concentration: 10–50 mg N/L) has occurred in areas with significant agricultural activities and small precipitation surpluses. Analysis of the model uncertainty also suggests that the nitrate export in most rivers is sensitive to the amount of nitrogen leaching from agricultural lands.

* *Corresponding author*. Center for Promotion of Interdisciplinary Education and Research, Educational Unit for Adaptation and Resilience for a Sustainable Society, Kyoto University, Kyoto, Japan.
E-mail address: hebin@flood.dpri.kyoto-u.ac.jp (B. He).
0043-1354/$ – see front matter © 2011 Elsevier Ltd. All rights reserved.
doi:10.1016/j.watres.2011.02.011

1. Introduction

Increasing world population has resulted in higher food and energy demand and consumption over the past half century (United Nations, 1996). Human activities have greatly accelerated and enlarged the natural cycles of nutrients and nitrogen in the soil, water, and atmosphere. Through activities such as fertilizer application, fossil fuel consumption, and leguminous crop production, humans have more than doubled the rate at which biologically available nutrients enter the terrestrial biosphere in comparison to pre-industrial levels (Galloway et al., 2004). One of the most important nutrients in this respect is nitrogen, which is an integral component of many essential plant nutrients. However, while nitrogen is an essential nutrient that plays important roles in increasing crop yields and quality, it is also a major pollutant in terrestrial ecosystems (Baker, 2003; Oenema et al., 1998; Schepers et al., 1995). Excess nitrogen used in fertilization has disturbed the biogeochemical nitrogen cycle of natural ecosystems, resulting in stratospheric ozone depletion, soil acidification, eutrophication, and nitrate pollution of ground and surface waters (Davis and Koop, 2006; Ding et al., 2006; Hantschel and Beese, 1997; Rijtema and Kroes, 1991). Water quality degradation associated with nitrate leaching from agricultural soils is an important environmental issue worldwide (Galloway, 1998, 2000; Galloway and Cowling, 2002; Galloway et al., 1995). Losses of nitrogenous compounds in the atmosphere and aquatic systems have inverse impacts not only on human health and global warming, but also on natural and agricultural terrestrial and aquatic ecosystems. The effects of agricultural diffuse source nitrogen pollution on water quality and aquatic ecosystems have received considerable research attention in recent years (Howarth et al., 2002; Hudson et al., 2005). Nitrogen pollution is one of the major pollutants, yet it is difficult to estimate because its sources are widely spread. In addition, both natural and anthropogenic emitters are responsible for nitrogen pollution (He et al., 2009a and 2009b). For example, natural reactions of atmospheric forms of nitrogen can result in the formation of nitrate and ammonium ions. In addition, the large anthropogenic sources of septic tanks, application of nitrogen-rich fertilizers, and agricultural processes have greatly increased the nitrate concentration, particularly in groundwater. Since the characteristics of each river basin is different, the relative contribution from each emitters has to be analyzed based on the database of land use, population, agricultural fertilizer, industrial production, livestock, etc.

To date, research on the nitrogen cycle has primarily focused on the river basin scale (Dumont et al., 2005; Seitzinger et al., 2005). Very few national- or global-scale studies exist (Dumont et al., 2005), and prediction of nitrogen export is still insufficient (Seitzinger et al., 2005). In addition, most large- or global-scale nitrogen studies have treated entire river basins as the basic unit and, as a result, the calculated nitrogen leaching or nitrate concentration mainly reflects the amount of nitrogen in river outlets (Bouwman et al., 2005a; Harrison et al., 2005; Howarth et al., 2002; He et al., 2009b). Detailed information on nitrogen leaching or nitrate concentration in individually distributed grids is lacking in the current literature. Furthermore, global nitrogen cycle models have relied on calculated amounts of nitrogen fertilizer application based on yearly statistical databases for each country. Monthly nitrogen fertilizer application amounts have not been available for global-scale study.

The aim of this study was to estimate the global nitrogen loading from point and nonpoint sources separately and apply an integrated biogeochemical model to nitrogen export for global rivers. The nitrogen fertilizer application amount and nitrate leaching were first calculated for each grid box, measuring 0.5° by 0.5°, using the process-based N-cycle model. In this article, we present an initial overview of the integrated modeling framework, including the structure, database, and model results. Section 2 presents the methodology, and Section 3 discusses the database for the point and nonpoint sources. The integrated simulation using the above model and database is discussed in Section 4.

2. Method

2.1. *Integrated modeling framework*

This study proposed an integrated biogeochemical modeling of global nitrogen loads from anthropogenic and natural sources. The global runoff was simulated by a land surface model driven by atmospheric forcing in an off-line mode (Fig. 1). Then, the nitrogen load (NL) from different sources such as crop, livestock, industrial plant, urban and rural population were calculated by applying datasets of fertilizer utilization, population distribution, land cover map, and social census. The number of livestock and population in each country was collected from national census database. The

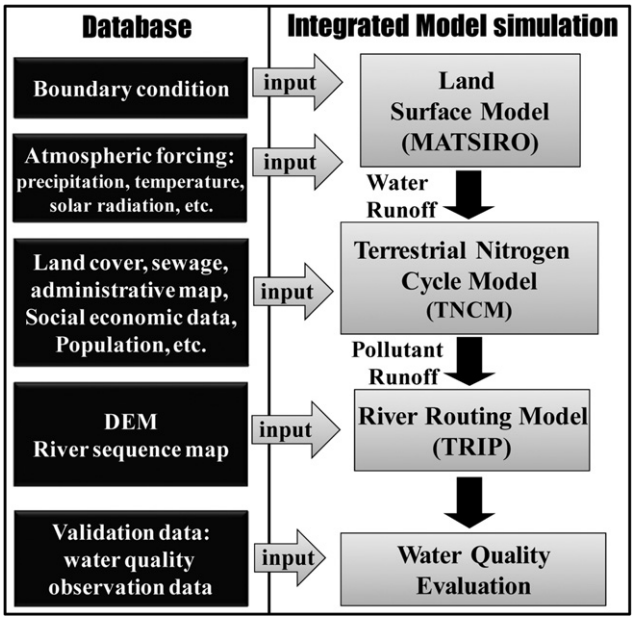

Fig. 1 – Integrated modelling framework for calculating global terrestrial nitrogen load and rivers' nitrogen concentration.

fertilizer consumption for each country were derived from FAO census database (FAOSTAT). The nitrate leaching from soil layers in farmland, grassland and natural conditions was calculated by using a terrestrial nitrogen cycle model (TNCM) (He et al., 2009a). A river routing model was used to transport nitrogen from natural and anthropogenic sources through river channels, as well as collect and route nitrogen to the river mouths. Subsequently, we will discuss the land surface model in Section 2.2, the terrestrial nitrogen cycle model in Section 2.3, the river routing model in Section 2.4, biological N fixation, atmospheric N deposition, and denitrification in Section 2.5, nitrate leaching in Section 2.6, and the design of the integrated simulation in Section 2.7.

2.2. *Land surface model*

Several land surface models have been developed for use in global or regional climate models (Sellers et al., 1996; Dickinson et al., 1998). These models incorporate radiation transfer, evaporation, transpiration, snow, runoff and also take into consideration the effects of vegetation. In the result, the energy and water exchange between the land and atmosphere is illustrated as a vertical one dimensional processes. In this study, we employed the Minimal Advanced Treatment of Surface Interaction and Runoff Model (MATSIRO) which is projected to be used for long-term simulations of climate studies (Takata, 2000, 2001; Takata et al., 2003). The MATSIRO model computes vertical energy and water fluxes in a grid cell based upon specifications of soil properties and vegetation coverage for each grid (Hirabayashi et al., 2005). It was used to estimate the long-term terrestrial water fluxes by long-term atmospheric forcing data that was stochastically estimated from monthly mean time series of precipitation and temperature (Hirabayashi et al., 2005, 2008). MATSIRO model has a single-layer albedo. The bulk exchange coefficients are evaluated based on a multilayer canopy model. The fluxes are calculated from the energy balance at the ground and canopy surfaces in both snow-free and snow-covered portions that consider the subgrid snow distribution. The snow has the variable number of layers from one to three in accordance with snow water equivalent (SWE), and the snow temperature is calculated by a thermal conduction equation. The snow mass is prognosticated from snowfall, snowmelt, refreezing of rainfall and snowmelt, and sublimation. The detailed description of snow process can be found in Takata et al. (2003). Evaporation of water on the canopy and transpiration parameterized on the basis of photosynthesis (Sellers et al., 1996) are included. A simplified TOPMODEL (Beven and Kirkby, 1979) calculates baseflow runoff, in addition to surface flows. The original TOPMODEL usually requires a detailed elevation data over the domain of interest, however, it is difficult to treat such data at a global scale. Therefore, in MATSIRO, the subgrid topography in a grid cell is roughly approximated as repetition of a slope with a uniform slope angle and with the distance between ridge and valley (Takata et al., 2003). There are five soil layers in which energy and water movements are treated with physical equations that consider freezing and condensation. The model is originally designed as a land surface sub-module of an atmospheric general circulation model (AGCM). The coupled model appropriately reproduced the observed seasonal cycles of the energy and water balance at both regional (Hawaiian Islands: Sakamoto et al., 2004; Japan: Sakimura, 2007) and global scale (Hirabayashi et al., 2008). The model is also driven by atmospheric forcing in an off-line mode. Model application results in an off-line mode are described in previous studies such as Hirabayashi et al. (2005). This study used runoff output of off-line simulation of MATSIRO as an input of a nitrogen cycle model.

2.3. *Terrestrial nitrogen cycle model*

The TNCM (Fig. 2) is developed to consider the mass balance of nitrogen in vegetation and organic soil of the ecosystem. It is based on the original model by Lin et al. (2000, 2001). The ecosystem was divided into an atmospheric and a terrestrial reservoir. The terrestrial nitrogen cycle consists of biological processes that depend on a variety of the environmental factors. The model contains five variables as for nitrogen: nitrogen in vegetation (N_{veg}, unit: ton N km^{-2}), organic N in detritus (N_{det}, unit: ton N km^{-2}), organic nitrogen in humus (N_{hum}, unit: ton N km^{-2}), ammonium (N_{amm}, unit: ton N km^{-2}), and nitrate (N_{nit}, unit: ton N km^{-2}). The nitrogen balance for each process was shown as below (He et al., 2009a):

$$\frac{\partial N_{veg}}{\partial t} = n_{uptake} - n_f(1 - hvst) + n_{fix} \tag{1}$$

$$\frac{\partial N_{det}}{\partial t} = n_f - n_{dm} - n_{dh} \tag{2}$$

$$\frac{\partial N_{hum}}{\partial t} = n_{dh} - n_{hm} + fert\_hum + lst \tag{3}$$

$$\frac{\partial N_{amm}}{\partial t} = n_{dm} + n_{hm} + n_{ammd} - n_{uptake} \times \frac{N_{amm}}{N_{amm} + N_{nit}} - n_{nitrif} - n_{vola} + fert\_amm \tag{4}$$

$$\frac{\partial N_{nit}}{\partial t} = n_{nitrif} - n_{nitrgas} + n_{nitd} - n_{uptake} \times \frac{N_{nit}}{N_{amm} + N_{nit}} - n_{denitr} - n_{leach} + fert\_nit \tag{5}$$

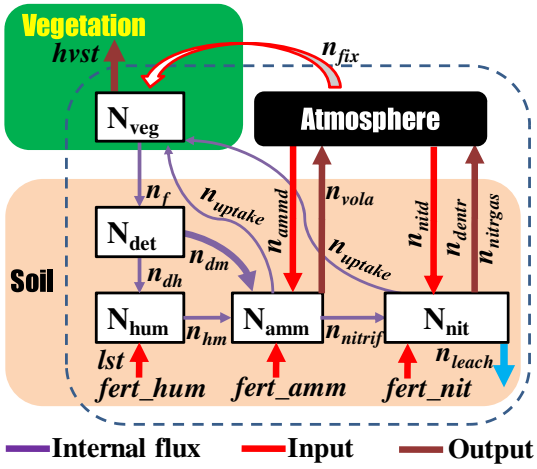

Fig. 2 – Flow chart for the terrestrial nitrogen cycle model (He et al., 2009a). The variables in this figure are described in the text, Section 2.3.

Where, *nuptake* is flux of nitrogen uptake by plant (ton N km^{-2} day^{-1}), *nf* is flux of litter-fall from leaf, trunk, and root as in nitrogen (ton N km^{-2} day^{-1}), *nfix* is flux of nitrogen fixation as in nitrogen (ton N km^{-2} day^{-1}), *ndm* is flux of detritus mineralization as in nitrogen (ton N km^{-2} day^{-1}), *ndh* is flux of detritus huminification as in nitrogen (ton N km^{-2} day^{-1}), *nhm* is flux of humus mineralization as in nitrogen (ton N km^{-2} day^{-1}), *nammd* is flux of nitrogen deposition as in ammonium (ton N km^{-2} day^{-1}), *Namm* is potential nitrogen storage as in ammonium (ton N km^{-2}), *Nnit* is potential nitrogen storage as in nitrate (ton N km^{-2}), *nnitrif* is flux of nitrification (ton N km^{-2} day^{-1}), *nvola* is flux of ammonia volatilization (ton N km^{-2} day^{-1}), *nnitrgas* is flux of gaseous emissions during nitrification process (ton N km^{-2} day^{-1}), *nnitd* is flux of nitrogen deposition as in nitrate (ton N km^{-2} day^{-1}), *ndenitr* is flux of denitrification (ton N km^{-2} day^{-1}), *nleach* is flux of nitrate leaching (ton N km^{-2} day^{-1}), *fert_hum* is the amount of fertilizer in humus (ton N km^{-2} day^{-1}), *fert_amm* is the amount of fertilizer in ammonium (ton N km^{-2} day^{-1}), *lst* is the amount of fertilizer from livestock (ton N km^{-2} day^{-1}), *hvst* is the ratio of harvested crops. For natural ecosystem, all of fertilizer amount i.e., *fert_hum*, *fert_amm*, and *lst* equal to zero (He et al., 2009a).

The mathematical formulas describing all these processes and parameters in detail can be found in Lin et al. (2000, 2001) and He et al. (2009a). Most of the parameter values required in this model were either cited from reference papers or determined by model calibrations as described in Lin et al. (2000).

2.4. River routing model

The aim of river routing model is to give directions for lateral water and pollutant movement by creating an idealized network of river channels. In this study, Total Runoff Integrating Pathways (TRIP) (Oki et al., 1999; Oki and Sud, 1998; Ngo-Duc et al., 2007) was employed to transport water and nitrogen flow through channels. The source of global digital elevation map (DEM) is ETOPO5 (Edwards, 1986). The basin delineation data used in this study have a spatial resolution of 0.5° by 0.5°. It was used to transport nitrogen from natural and anthropogenic sources through river channels, as well as collect and route nitrogen to the river mouths. Amounts of total nitrogen (TN) in direct runoff, lateral subsurface flow and percolation are estimated as the products of the volume of water and the average concentration. Transport or retention factors are taken into account through routing of water and nitrogen in the river flow via transmission losses (He et al., 2009a). Since dissolved inorganic nitrogen (DIN) is often the most abundant and bioavailable form of N and contributes significantly to coastal eutrophication (Veuger et al., 2004), we calculated DIN input into rivers from point sources by multiplying the amount of TN with an estimated fraction of TN that is DIN in sewage effluents (Dumont et al., 2005) as below:

$$\mathrm{DIN} = \mathrm{TN}\cdot[0.485 + T_N\cdot 0.255/\max(T_N)] \quad (6)$$

where, T_N is a country by country fraction of TN removed by wastewater treatment compiled by Bouwman et al. (2005a), 0.485 is an estimate of the fraction of TN that is DIN in sewage effluent (Seitzinger, 1995), and 0.255 is the maximum increase in DIN to TN ratio that can be achieved by sewage treatment (Seitzinger, 1995). A detailed explanation can be found in Bouwman et al. (2005a) and Dumont et al. (2005). The time resolution of TRIP simulation was set as 1.0 day in this study.

2.5. Biological N fixation, atmospheric N deposition, and denitrification

Biological N fixation of atmospheric N in natural ecosystems was estimated by using TNCM. It was assumed to be the sum of symbiotic and nonsymbiotic fixations, which can be modeled by the function in Lin et al. (2000), as shown in the equation below.

$$n_{fix} = n_{fix\_sy} + n_{fix\_nsy} \quad (7)$$

where, n_{fix} is flux of nitrogen fixation as in total nitrogen (ton N km^{-2} day^{-1}), n_{fix_sy} is nitrogen symbiotic fixation (ton N km^{-2} day^{-1}), n_{fix_nsy} is nitrogen nonsymbiotic fixation (ton N km^{-2} day^{-1}).

Nitrogen deposition includes dry and wet deposition of ammonia gas, nitrate, and nitrogen compounds from the atmosphere to soil by rain, snow, and dust. The deposition of ammonium and nitrate was modeled by using the method in Lin et al. (2000), where wet deposition was modeled as a linear function of precipitation (Hudson et al., 1994).

Nitrogen discharging from land surface to rivers was assumed to infiltrate through soil where some fraction was removed by denitrification and organic matter accumulation. The surplus nitrogen flows to the river and then to the sea, were analyzed in conjunction with precipitation surplus. In this study, nitrogen was assumed to be denitrified and accumulated in the soil by a first-order reaction expressed in Shindo et al. (2003) and He et al. (2009a).

$$C = C_0\exp(-k_T\cdot t_R) \quad (8)$$

$$k_T = 2^{(T-20)/10}\cdot k_{20} \quad (9)$$

where, C_0 indicates the original nitrogen concentration (mg/L), k_T and k_{20} are coefficients of denitrification and accumulation at T and 20 ($k_{20} = 3.0$), respectively, and t_R is residence time in soil (day).

2.6. Nitrate leaching

Many different models are used for the detailed simulation of the average nitrate leaching and denitrification process (Brisson et al., 2003; Johnsson et al., 1987; Shaffer et al., 1991). However, such models are too detailed for the 0.5° by 0.5° resolution and these models require data on environmental conditions (i.e., daily condition of root growth, phenology stage, crop yield, leaf area index, etc.) and agricultural management (i.e., irrigation option, drainage option, precise planting and cultivation date, fertilizer application), which are not available on the spatial scale of our model. In the present stage of this study, the TNCM was applied to estimate nitrate leaching from natural ecosystems such as grassland and forest with fertilizer application rate as zero. Furthermore, it was used to estimate nitrate leaching from croplands with the application of fertilizer amounts. The nitrate leaching is

strongly related to soil water content, soil texture, and NO_3^- concentration. For modeling the nitrate leaching flux, the below equation was employed (He et al., 2009a):

$$N_{leach} = N_{nit} \cdot \frac{R_t}{\theta_s} \cdot 10^3 \quad (10)$$

Where, N_{leach} is the flux of nitrate leaching (ton N km^{-2} day^{-1}), N_{nit} is potential nitrogen storage as in nitrate (ton N km^{-2}) which was calculated by TNCM model, R_t is runoff (tonne km^{-2} day^{-1}) which was calculated by MATSIRO model, and $\theta_s$is soil water storage (mm) which was calculated by MATSIRO model (He et al., 2009a).

2.7. Design of the integrated simulation

The integrated modeling framework for calculating global terrestrial nitrogen load and river's nitrogen concentration is illustrated in Fig. 1. The model operates on a daily time step and at a spatial resolution of 0.5° by 0.5° over the world. After the input datum are read from files, the three-step modeling procedure is applied. First, water discharge, nitrogen balance, and nitrate leaching are calculated for each grid (0.5° by 0.5°) by the MATSIRO and TNCM. Then the outputs from each grid (e.g. lateral water flows, nitrate flow) are summed with point pollution load (e.g. from industrial source, sewage plant). Finally, the routing procedure TRIP is applied to transport point and nonpoint pollution along rivers, taking transmission losses into account. Among these, the hydrological module is fundamental for all the modeling systems in this study. It was tested and validated in Hirabayashi et al. (2005, 2008). It reproduces well the observed seasonal cycles of the energy and water balance.

In addition, before commencing a long-term nitrogen cycle simulation, it is usually necessary to allow the land surface to adjust to a steady-state. Some groups have nevertheless apparently used spin-up techniques successfully to initialize the ocean state for long climate studies (Manabe et al., 1991,, 1992; Stouffer et al., 1994; Thornton and Rosenbloom, 2005; Lin et al., 2000). The objective of spin-up is to bring the model close to a steady-state so that negligible climate drift is experienced in the control run which follows. In this study, the spin-up procedure with a time step of 1 day was used for 100-year spin-up period.

3. Data

Most of the available input database, which was used in global river nutrient export models, and the available model validation all choose 1995 as the base year. Therefore, the initial database constructed in this study is also based on the year 1995 as an example. All the input datasets have a spatial resolution of 0.5° by 0.5°. The following section will describe the detailed information about the database used in this study (Table 1).

3.1. Hydrometeorological database

Air temperature, precipitation, short wave downward radiation with the spatial resolution of 1° by 1°and the temporal resolution of one day are from the second Global Soil Wetness Project (GSWP2; Dirmeyer et al., 2006) database. The soil temperature, soil water content, and runoff are calculated and validated by MATSIRO model (Hirabayashi et al., 2005) at the spatial resolution of 1° by 1°and the temporal resolution of one day. All the input data were divided into the same spatial resolution of 0.5° by 0.5° (allocation of the same value in four 0.5° grids within 1° grid) and the dataset in 1995 was used in this study since the final validation and model evaluation are all based on this year.

3.2. Land cover map

The land cover map was generated from the database of GLCC (USGS). Its original spatial resolution is on a 30 s grid (Loveland et al., 2000). In this study, the spatial resolution of 0.5° has been applied for TNCM, LSM and RRM. Therefore, in each 0.5° grid, the area ratio of each land cover was calculated and

Table 1 – Overview of data used in this study.

Data	Spatial Resolution	Temporal resolution	Data period	Source
Land cover map	0.5°	–	2000	http://edc2.usgs.gov/glcc
Digital elevation map	0.5°	–	–	Oki and Sud, (1998)
Basin delineation map	0.5°	–	–	Oki and Sud, (1998)
River routing map	0.5°	–	–	Oki and Sud, (1998)
Soil temperature, moisture	1°	Daily	1995	Hirabayashi et al. (2005)
Precipitation, Air temperature, Solar radiation	1°	Daily	1995	Hirabayashi et al. (2005)
Runoff	1°	Daily	1995	Dirmeyer et al. (2006)
Ammonia fertilizer	0.5°	Yearly	1995	FAOSTAT
Nitrous fertilizer	0.5°	Yearly	1995	FAOSTAT
Crop calendar	1°	Yearly	1995	Hanasaki et al. (2008)
Global population map (urban, rural, total)	0.5°	Yearly	1995	Bengtsson et al. (2006)
Manure N addition	0.5°	Yearly	1995	Bouwman et al. (2005a)
Sewage point sources	0.5°	Yearly	1995	Bouwman et al. (2005a)
DIN load	River basin	Yearly	1995	Dumont et al. (2005)

accumulated from the 30 s grid. The land cover data were reclassified among cropland, grassland, forest, water wetland, tundra, and other land. The area of each land cover type in each 0.5° by 0.5° cell was then calculated.

3.3. Nitrogen load estimation

The spatial and temporal distributions of on-ground N fertilizer use from various crops and agricultural practices were quantified in this study (Fig. 3). The assessment of on-ground N fertilizer due to multiple land use activities can be complex and the traditional method is to only use the national census data without considering the crops' spatial distribution, fertilization and harvest patterns. In this study, the monthly fertilizer application rates in the world were calculated by using global fertilizer statistics data and each crop's agricultural manuals (FAOSTAT). Then, the land cover map showing the spatial distribution of areal ratio of each crop in each grid with a spatial resolution of 0.5° by 0.5° was generated for the whole global land surface. Finally, the spatial distribution map of fertilizer utilization with a temporal resolution of one month was generated. The crop distribution map was generated from the crop area. Then, the fertilizer amount for different land cover was calculated in each grid (Fig. 4). The nitrogen load from livestock was calculated for various livestock species based on literature values (Bouwman et al., 2005a, 2005b) by using the animal numbers and pollutant emission load per animal.

Point sources of N are primarily associated with human excreta and industrial water use (wastewater drainage). As for the calculation of nitrogen load from domestic water use for populations provided with sewage plants, the database of diffusion rate of public sewerage and population distribution was utilized. The distribution of population provided with wastewater service was calculated by using the database of population without sewage plants and population with wastewater service. Generally, the population without sewage plants is distributed in rural area and the population with sewage plants is distributed in urban area. As for the calculation of nitrogen load from industrial water use, this was calculated by using the database of the production of pollutant emission basic unit of industrial classification. The distribution of nitrogen load from industry can then be calculated by land cover data and nitrogen load. Furthermore, the distribution of sewage diffusion rate was calculated from total population distribution and population without sewage plants. The nitrogen load from industrial water use was calculated by the distribution of nitrogen load from industry and the distribution of sewage diffusion rate (Bouwman et al., 2005a; He et al., 2009a). DIN input into rivers from point sources was estimated by the method proposed by Dumont et al. (2005). Total nitrogen (TN), was used to calculated DIN from human excreta and industrial wastewater in sewage effluents by multiplying the amount of TN with an estimated fraction of TN and DIN, which was described in Equation (6).

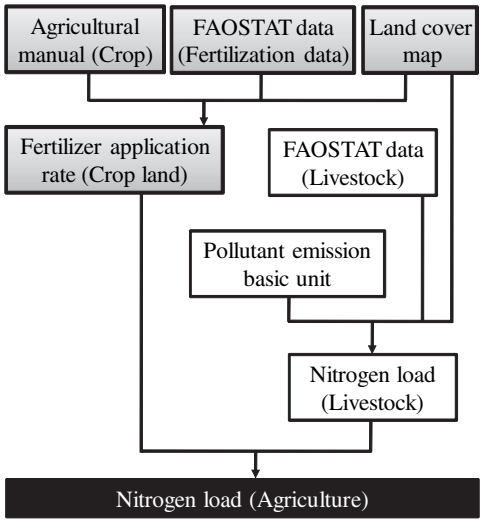

Fig. 3 – Flow chart for the calculation of nitrogen load from agricultural sources.

3.4. Validation data collection

Nitrogen has many chemical forms and compounds, which are very mobile and dynamic both in space and time. In addition, biogeochemical modeling of nitrogen cycle at the global or national scale with large grid cells usually only consider the vertical flows. In this study, the lateral flows are included by using the routing procedure of TRIP in the modeling system so that the chemical fluxes at the global scale can be validated using the data of measurements at the river outlet. For nitrogen cycle and routing model's validation, we collected the observed dissolved inorganic nitrogen (DIN) concentration in major global rivers from literature records, which are published values and available for open access. Table 2 shows all selected 61 rivers for model validation (Alexander et al., 1996; EEA, 1998; Dumont et al., 2005; Seitzinger et al., 2005; Van Drecht et al., 2003).

4. Result and discussion

4.1. Model validation

Firstly, the land surface model was run to obtain a steady-state model. The global nitrogen cycle model restarted after an annual simulation, with the output used as the new initial conditions for the next year. The experiment began with a 100-year spin-up of the model, forced by the repeated initial annual nitrogen cycle and climatological data. After spin-up was completed, a steady-state of global nitrogen storage could be obtained. Then, the modeled annual dissolved inorganic nitrogen (DIN) load (ton N y^{-1}) at each river was compared with the existing data of observed DIN load. As for the hydrological model results, the long-term terrestrial water fluxes were estimated well using the land surface model driven by long-term atmospheric forcing data (Hirabayashi et al., 2005). High correlations between predicted and observed annual runoff were obtained at many basins globally, but correlations are low in dry areas and in cool-temperate zones. Moreover, annual snow covered area in North America and northern Europe and annual summer soil moisture in Mongolia were successfully replicated by the model (Hirabayashi et al., 2005).

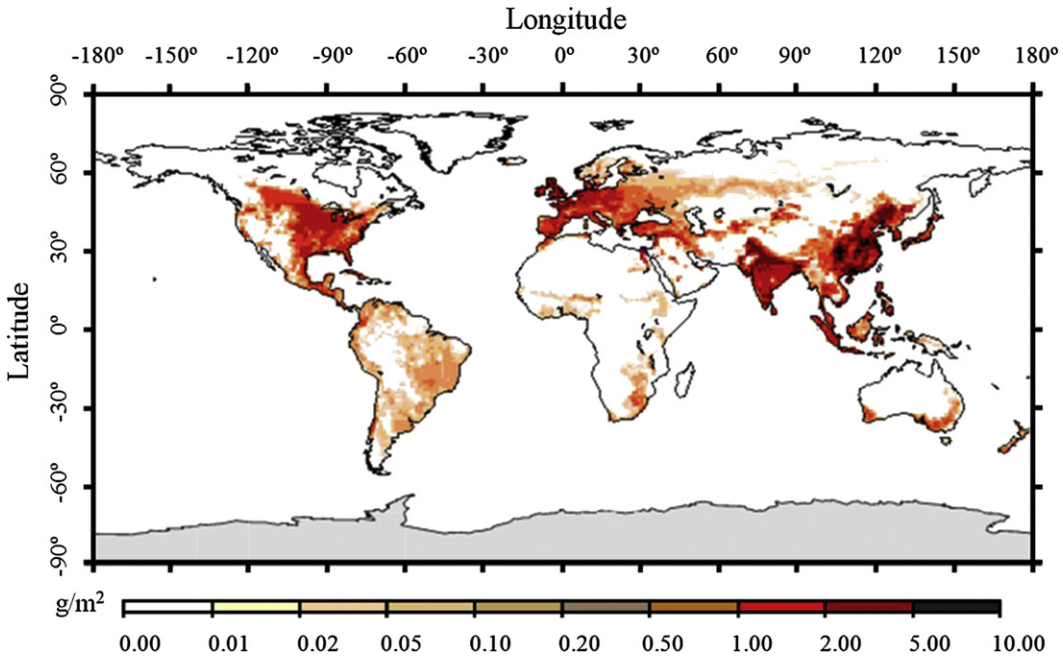

Fig. 4 – Map of global annual nitrogen fertilization use in 1995.

The predicted annual DIN yield (ton N km^{-2} y^{-1}), calculated by dividing the annual DIN export by the river basin area, was also compared with the measured yield. Fig. 5 shows a scatter plot of calculated and observed (Dumont et al., 2005) DIN load and yield for the selected 61 rivers in 1995. The figure shows a linear relationship between the logarithms of observed and modeled annual values of DIN load and yield. The regression lines between observed and predicted DIN load and yield are very close to a 1:1 ratio. The model efficiencies (R^2, the coefficient of determination) were 0.88 and 0.81 for DIN load and yield, respectively. Consequently, we can conclude that the model reproduced the DIN load in selected rivers with reasonable accuracy.

Fig. 6 shows calculated and observed DIN load and yield for the selected 61 rivers in this study. The *x*-axis is the river ID from Table 2; rivers are ordered in size from the largest (Amazon) to the smallest (Pee Dee) basin. From the top figure in Fig. 6, we can see that the DIN load in most of the rivers is proportional to the size of the river basin. However, some river basins with larger areas have smaller DIN loads, such as the Murray River (ID = 10) in Australia and Rio Grande (ID = 13) in North America, which have relatively smaller river discharge. In Table 2, we can find some river basins in which the DIN loads are smaller than 1.5 10^3 ton/year. As shown in the bottom figure in Fig. 6, the DIN yield in these two rivers is very small; this is because the DIN yield is calculated by dividing the DIN export by the river basin area. Among the 61 rivers, the river with the largest DIN yield is the Rhine River (ID = 24). From Fig. 6, we can see that the model used in this study reproduced DIN yield and load well for most of the selected 61 rivers, which have different spatial locations and basin sizes.

Fig. 7 illustrates the correlation of river discharge with DIN load and DIN yield for selected rivers in the world. The logarithm–logarithm relationship in Fig. 7 shows that river discharge has stronger correlation with DIN load than DIN yield. It means increased river discharge generally exerts a positive effect on DIN load in rivers at a long term (one year) time scale. At higher annual flows, rivers deliver more nitrogen from upstream to downstream by reducing residence times. However, as for DIN yield, its correlation with river discharge will be more complicated since DIN yield is also affected by the catchment characteristics, such as area, elevation, time and distance of transport for nitrogen in a drainage network. Because river discharge is correlated with vegetation, the relationship between DIN yield and river discharge corresponds to a relationship between DIN yield and vegetation type (Lewis et al., 1999).

4.2. *Annual nitrate leaching from terrestrial ecosystems*

Fig. 8 presents a map of annual nitrate leaching from the terrestrial ecosystem in 1995. The range of nitrate leaching was very large across the world. Similar to the results from Dumont et al. (2005), higher nitrate leaching was predicted for tropical humid-climate river basins (i.e., in Indonesia, West Africa, the Amazon, and the Zaire River basin), densely populated basins with high GDP (i.e., Rhine and Thames river basins), and basins with extensive agricultural activities (i.e., Yangtze and Ganges river basins). Other areas with high values were predicted in New Zealand and Japan. The lowest nitrate was predicted for basins with low population density such as most basins at high latitudes and also for arid regions (i.e., Nile River basin and Tamanrasett River basin). In this paper, nitrate was calculated by the terrestrial nitrogen cycle model, for which the main input data included simulated runoff, fertilizer application, and precipitation. Therefore, the predicted nitrate was greatly influenced by these input data and the resulting spatial pattern was very similar to those of

Table 2 – Selected global rivers for model validation.

ID	Name	Continent	Area (10^4 km^2)	Average Q(km^3/yr)	Pop. density (person/km^2)	Agriculture land (%)	DIN load (10^3ton)
1	Amazon	S. A.	583.30	5025.75	4.39	8.62	1006.19
2	Mississippi	N.A.	319.10	538.37	22.47	74.69	815.62
3	Ob	Asia	301.50	289.73	10.14	37.23	295.47
4	Parana	S. A.	265.40	595.59	27.80	59.47	116.51
5	Yenisei	Asia	256.90	423.42	3.06	13.65	110.72
6	Lena	Asia	243.30	284.92	0.56	0.00	51.34
7	Yangtze Jiang	Asia	178.80	436.57	244.07	69.34	585.57
8	Amur	Asia	174.80	261.14	36.37	26.78	139.32
9	Indus	Asia	113.90	38.37	169.23	37.02	155.93
10	Murray	Australia	102.80	20.46	3.51	53.89	1.13
11	Yellow	Asia	89.05	18.46	158.88	81.50	107.31
12	Yukon	N.A.	85.27	42.4	0.13	0.00	26.09
13	Rio Grande	N.A.	80.19	6.53	17.45	73.85	0.48
14	Columbia	N.A.	72.93	198.21	9.19	17.40	54.04
15	Kolyma	Asia	66.32	67.57	0.09	0.00	11.94
16	Don	Europe	42.16	33.42	48.60	98.70	8.05
17	Pearl	Asia	40.71	142.01	207.09	69.11	213.04
18	Pechora	Europe	31.31	78.54	1.79	0.00	20.26
19	Churchill	N.A.	30.24	46.09	0.21	4.75	2.87
20	Neva	Europe	28.35	71.34	28.31	2.33	21.01
21	Yana	Asia	22.42	17.21	0.04	0.00	5.81
22	Rufiji	Africa	18.61	62.53	23.92	54.02	51.34
23	Wisla	Europe	18.00	22.64	135.49	50.97	66.92
24	Rhine	Europe	16.45	58.47	300.35	45.99	361.97
25	Elbe	Europe	14.80	16.61	166.61	53.68	117.72
26	Brazos	N.A.	12.46	5.45	27.57	85.11	6.98
27	Balsas	N.A.	12.26	31.83	230.44	37.64	8.96
28	Colorado	N.A.	12.08	3.88	16.04	81.81	2.92
29	Odra	Europe	11.94	11.42	121.44	63.49	46.54
30	Kuskowin	N.A.	11.54	14.66	0.07	0.00	15.80
31	Anabar	Asia	9.86	7.3	0.00	0.00	1.15
32	Nemanus	Europe	9.66	16.76	46.26	37.55	13.37
33	Penzhina	Asia	8.55	18.11	0.09	0.00	2.18
34	Daugava	Europe	8.32	16.17	30.57	20.72	12.58
35	Mezen	Europe	7.54	18.65	1.84	0.00	1.87
36	Seine	Europe	7.32	9.75	210.31	81.63	99.90
37	Tejo	Europe	7.31	8.67	101.42	57.97	8.98
38	Susquehanna	N.A.	7.19	25.44	53.55	23.14	35.44
39	Bug	Europe	6.90	5.64	74.05	84.09	1.95
40	Usumacinta	N.A.	6.79	100.25	36.12	30.35	38.17
41	Copper	N.A.	6.70	31.75	0.08	0.00	21.79
42	Kuban	Europe	6.36	19.74	66.84	61.20	21.06
43	Paraiba do Sul	S. A.	6.28	29.62	68.34	58.98	11.62
44	Sacramento	N.A.	5.87	26.16	16.88	15.51	2.24
45	Narva	Europe	5.80	11.26	19.66	30.58	4.25
46	Sakarya	Asia	5.68	4.42	105.59	66.67	8.81
47	Appalachicola	N.A.	5.47	27.44	79.56	25.88	12.85
48	Saint John	N.A.	5.29	32.67	8.46	7.81	3.16
49	Stikine	N.A.	5.12	22.4	0.04	0.00	11.92
50	Kamchatka	Asia	5.04	25.92	0.72	0.00	4.47
51	Trinity	N.A.	4.74	9.38	150.21	81.95	4.37
52	Glama	Europe	4.73	18.46	28.54	0.00	9.07
53	Weser	Europe	4.55	7.92	196.98	28.99	54.78
54	Hudson	North	4.31	19.27	172.40	5.22	16.41
55	Altamaha	N.A.	4.15	13.75	38.59	5.50	4.69
56	Potomac	N.A.	3.83	11.36	91.50	29.39	15.16
57	Nushagak	N.A.	3.53	7.3	0.05	0.00	3.72
58	Tornionjoki	Europe	3.45	7.54	1.60	6.47	0.31
59	Klamath	N.A.	3.21	12.78	7.83	6.73	2.28
60	Dalalven	Europe	2.98	8.39	11.44	0.00	1.69
61	Pee Dee	N.A.	2.76	8.57	72.75	27.34	6.06

Note: Rivers are sequenced by basin area. (S.A: South America; N.A: North America).

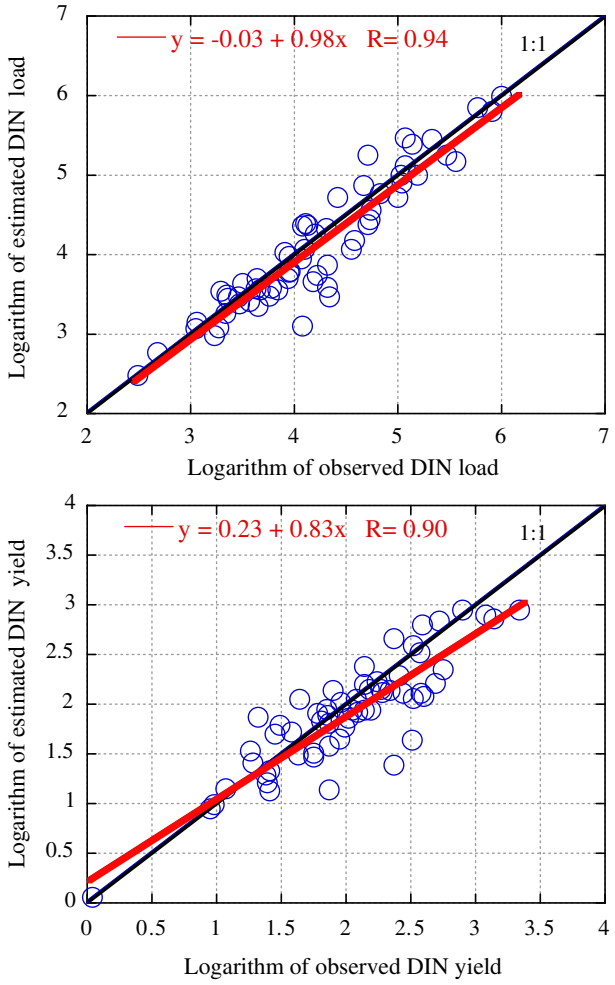

Fig. 5 – Scatter plot of comparison of calculated and observed DIN yield (ton N km^{-2} y^{-1}) and DIN load (ton N y^{-1}) for selected rivers. Dark diagonal line represents the 1:1 line.

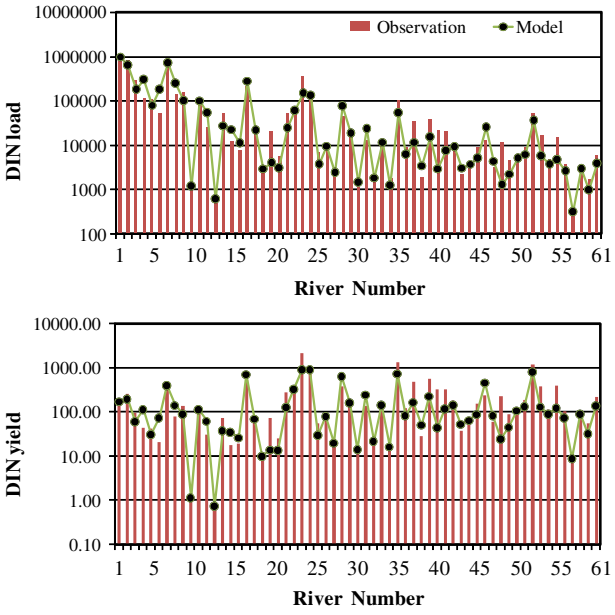

Fig. 6 – Comparison of calculated and observed DIN load (ton N y^{-1}) and DIN yield (ton N km^{-2} y^{-1}) for selected rivers.

runoff and fertilizer. Harrison et al. (2005) noted similar findings for the global distribution of dissolved organic nitrogen yield. As discussed by Seitzinger and Kroeze (1998) and shown in Fig. 8, Asia exports the most DIN to its coasts. This is due to its large surface area, high population, and large cultivated land area. The World Health Organization (WHO) has recommended healthy drinking water quality standards of 10 mg/L or less for nitrate–nitrogen, whereas most rivers in populated regions, according to the Global Environment Monitoring System (GEMS) database, have values about seven times this number at their mouths. The levels of dissolved nitrogen in these rivers are no longer due solely to natural processes such as weathering and soil organics, but also due to a substantial contribution by human activities, particularly in Asia (Subramanian, 2004; Jacks and Sharma, 1983).

4.3. *Spatial distribution of global nitrate–nitrogen concentration*

To identify where the nitrogen pollution is most serious, Fig. 9 shows the spatial distribution of the nitrate–nitrogen concentration in global rivers in 1995. The nitrate–nitrogen concentration is generally low for areas with low temperature and little precipitation. By contrast, the nitrate–nitrogen concentration becomes especially high in the eastern United States, the Rhine River, the Thames River, the lower portion of the Amazon River, the Yellow River and Yangtze River, northeast China, the east coast of the North China Plain, and some parts of the Republic of Korea and Japan. In comparing the maps of nitrogen fertilizer, nitrate leaching, and nitrate concentration, it is evident that, in specific areas, high nitrogen fertilizer use does not necessarily correspond with equally high nitrate leaching and nitrate concentration. This is apparent in the upstream region of the Yangtze River, upstream region of the Yellow River (China), upstream region of the Mississippi River (U.S.A), Murray River (Australia), Nelson River (Canada), and upstream region of the Danube River (Germany, Austria, Slovakia), midstream region of the Amur River (Russia, China). Conversely, other areas have relatively low nitrogen fertilizer use but high nitrate leaching and concentration. This is seen in places such as downstream region of the Amazon River, and the midstream region of Congo River. The processes of the nitrogen cycle are complex and nitrate leaching from soil layers is controlled by nitrogen load input, hydrometeorological conditions, and management practices. However, from a global perspective, the most serious nitrogen pollution has occurred in distinct areas exhibiting extensive agriculture and low precipitation surpluses (Shindo et al., 2003). This is visible from Fig. 7 in which large values of nitrate concentration (10–50 mg N/L) were found in the Northern plains of China, Northern India, and North-western portions of the U.S.A. In the groundwater of Shandong Province, China, for example, the average measured nitrate concentration was found to be 38.5 mg N L^{-1} and maximum concentration could exceed 100 mg N L^{-1} (Shindo et al., 2006).

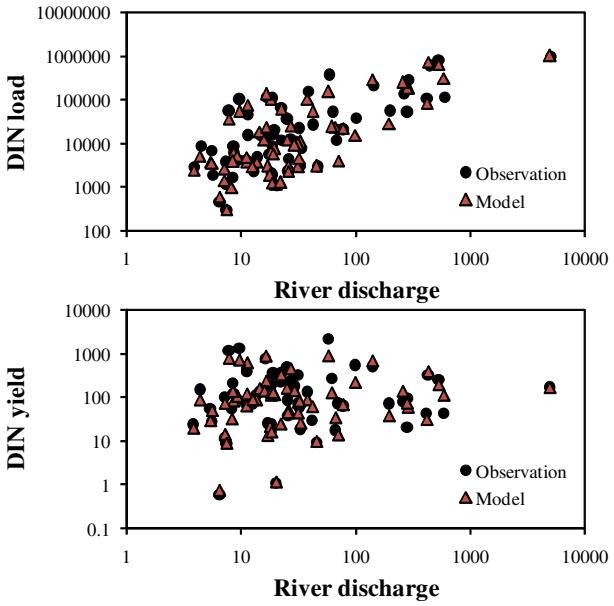

Fig. 7 – Correlation of river discharge ($km^3 y^{-1}$) with DIN load (ton N y^{-1}) and DIN yield (ton N $km^{-2} y^{-1}$) for selected rivers.

4.4. *Uncertainty analysis*

From the model results and analysis in the above sections, we can see that a degree of discrepancy remains between simulated and observed values of both nitrate–nitrogen flux and nitrate–nitrogen yield. The most likely causes originate from the uncertainties and variables inherent to the dataset, and model limitation. For example, as the main input to nitrogen loading on a global scale, nitrogen fertilizer usage has a large impact on the final calculation of nitrate leaching. The calculated nitrogen fertilizer value was compared with that of FAO census data. However, since census datasets are inevitably prone to a level of error, this data also contains some uncertainties surrounding their reported values. Nitrogen produced from livestock was calculated from the number of animals and excretion rate per head (Bouwman et al., 1997; Shindo et al., 2003). All the animals were considered to be full grown. For nitrogen deposition data, the simple empirical relationship between nitrogen deposition and precipitation was employed. However, long-term transport of nitrogen compounds, particularly NO_x, is important and thus for more precise estimation a transport model is needed (Shindo et al., 2003). For denitrification and organic matter accumulation in the soil, a simple reaction model considering temperature and residence time was applied. Nitrogen removal due to in-stream nitrogen retention is affected by complex conditions, which also creates uncertainty.

In addition, we collected the available observed DIN concentration data in major rivers from literature record for model validation. However, the observed data itself has uncertainty related to discharge measurement, sample collection (location and frequency), sample storage, and laboratory analysis. Moreover, data processing can contribute uncertainty to measured data because of missing data, assumptions made to estimate missing values, and mistakes in data management and reporting (Harmel et al., 2006). Therefore, to reduce the effect from the uncertainty of measured data, the frequency of water quality sampling for the collected data in this study commonly ranges from quarterly to monthly, with differences occurring by network, constituent, and time period. The dataset collected in this study was restricted to include only long term (>4 years) annual averages with at least 85% of the measurements taken between 1990 and 1997 (Dumont et al., 2005). The collected datasets also include world river basins with a broad range of area, land cover, climate, and topography (Table 2).

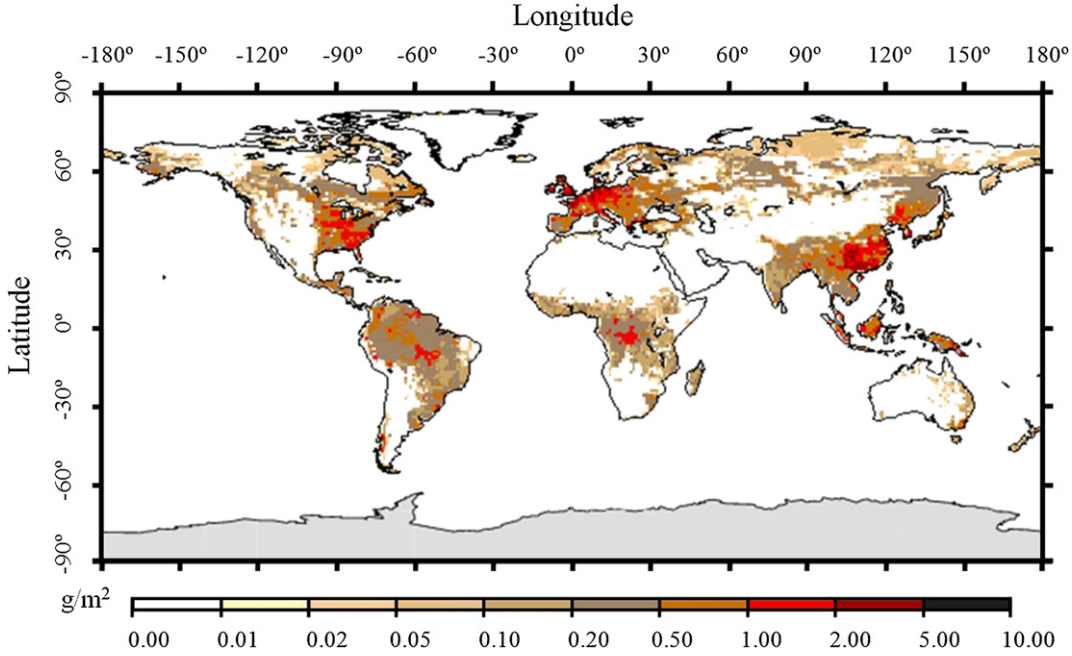

Fig. 8 – Simulated annual NO_3–N leaching from the terrestrial ecosystem in 1995.

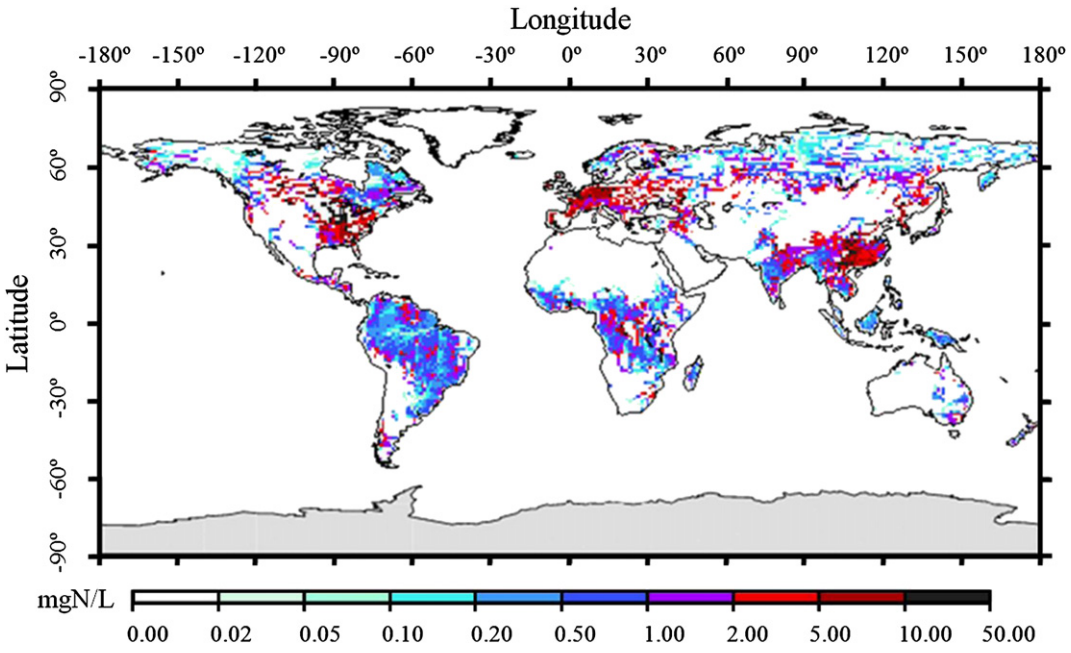

Fig. 9 – Map of simulated global NO_3–N concentration in 1995.

To assess the model uncertainty, five scenarios were considered in which the nitrogen load was increased by 10% for nitrogen leaching from the agricultural soil layer, nitrogen load from manure, nitrogen load from nitrogen fixation in agricultural lands, nitrogen load from nitrogen deposition in agricultural land, and nitrogen from sewage, respectively. The upper part of Fig. 10 presents the resulting ratios of simulated annual nitrate export under these five scenarios. The average nitrate–nitrogen export in 1995 is shown in the bottom part of Fig. 10 in comparison to the absolute nitrate–nitrogen export in different rivers. The figure shows that the contribution of nitrogen leaching from the agricultural soil layer is the most sensitive source for most of the selected 61 rivers. The second largest source is the nitrogen from sewage, followed by the nitrogen contribution from manure. The contributions of nitrogen deposition and nitrogen fixation in agricultural lands are nearly identical. These results indicate that the nitrate–nitrogen export in most rivers will be sensitive to the amount of nitrogen compounds leaching from agricultural soil layers and urban sewage. The nitrogen leaching from the agricultural soil layer is substantially affected by agricultural activities such as nitrogenous fertilizer application. Accordingly, the uncertainty from fertilizer application will have the largest impact on the estimation of nitrate–nitrogen export in rivers.

4.5. *Discussion*

The models in this study were constructed to examine dissolved nitrogen forms in particular. Through this emphasis, hydrological pressures, such as the positively correlated relationship between N export and runoff rate, contributing to the diffusion of anthropogenic and natural nitrogen sources could be incorporated (Seitzinger et al., 2005). The transport of nitrogen was only considered from the land surface into rivers and then out to sea. Transport of nitrogen in groundwater and interaction between river water and groundwater were not investigated in this study. Furthermore, the observed data for DIN concentration were collected at the outlet of each river. However, estimates of the absolute values of nitrogen concentration in river water involved uncertainties because sufficient data was not available for the ratio of total nitrogen export to nitrate export. This ratio would vary spatially according to temperature, river discharge, catchment characteristics, etc. (Shindo et al., 2003). Consideration of these factors would likely result in improved estimates.

Despite the limitations described above, we can still obtain good insight and estimates from the nitrogen-loading simulation at the global scale, which can improve our understanding of global spatial patterns and the magnitudes of nitrogen export from global river basins. In addition, the nitrogen model used in this study was specifically developed to obtain nitrogen export from river basins at the global scale. Similar to other global biogeochemical models, it differs in its degree of spatial resolution and mechanism formulation from models specifically developed for use in individual watersheds such as the Riverstrahler model (Billen et al., 1999; Seitzinger et al., 2005). Moreover, the current global nitrogen model is a process-based model considering the major process of nitrogen fixation, nitrification, denitrification, immobilization, mineralization, leaching, and nitrogen taken by vegetation. The fertilizer application rate for major crops and nitrogen load from major livestocks in the world were calculated to be inputs of the model. As results, the nitrogen leaching from soil layers was calculated through the model. This is different with most of the other nitrogen models in which the pollutant emission basic unit is applied to estimate the nitrogen leaching from soil layers (Sferratore et al., 2005). Moreover, the models in this study can provide a detailed information of calculated nitrate–nitrogen leaching from the terrestrial ecosystem and

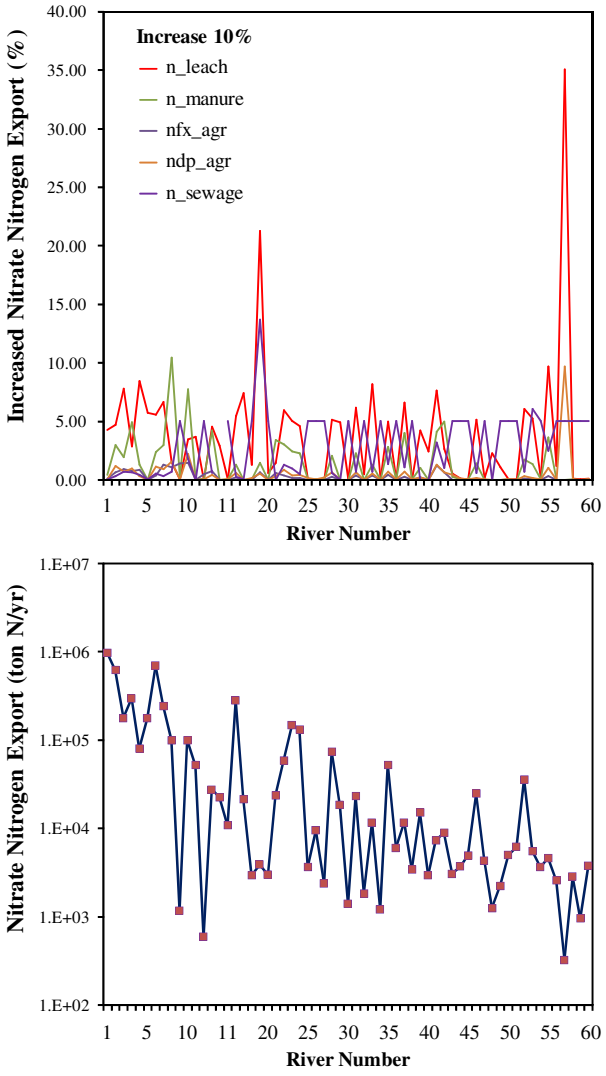

Fig. 10 – Annual NO_3–N export and ratios of simulated NO_3–N export under five scenarios in which the nitrogen load was increased by 10% for nitrogen leaching from the soil layer (n_leach), nitrogen load from manure (n_manure), nitrogen load from nitrogen fixation in agricultural land (nfx_agr), nitrogen load from nitrogen deposition in agricultural land (ndp_agr), and nitrogen load from sewage (n_sewage).

nitrate concentration in rivers not only at each river outlet, but also at each grid with a spatial resolution of 0.5° by 0.5°. Therefore, the nitrogen pollution condition in each grid of these river basins can be assessed accordingly. The calculated nitrogen loadings from agricultural lands, livestock, industrial plants, and domestic water use can provide useful databases for global-scale nitrogen pollution evaluation.

5. Conclusion

This paper has described integrated biogeochemical modeling of nitrogen load and its export to global rivers. The amount of nitrogen loading from various sources were calculated using datasets of fertilizer use, maps of land cover and population, social census data, and literature records. The nitrate leaching from soil layers in the terrestrial ecosystem was calculated using a global-scale terrestrial nitrogen cycle model. The model validation results indicate that discrepancy remains between simulated and observed DIN yield and load in some places. Uncertainties associated with the dataset and model limitations are the primary reasons for these discrepancies. However, this study aimed at understanding the spatial and temporal distribution of nitrogen load and it provided an initial overview of an integrated framework with which to estimate nitrogen load and nitrogen pollution in rivers at a global scale. As for future directions of related work, it is important to improve our understanding the mechanisms and time scales involved in the terrestrial response to nitrogen deposition, taking into account long-term nitrogen fertilization. The relationship between anthropogenic river water removal and DIN export is also required in future study. In addition, the same model architecture used in this study can be applied to a region (or several ones) with good data availability over several years to perform an in-depth test of the model. The database built in this study will provide a useful foundation for further model development and improvement, considering both anthropogenic and natural scenarios. As improved temporal and spatial resolution of validation datasets and the development of hydrological models that route materials downstream through river networks become available, it will be possible for us to further examine seasonal patterns and finer spatial resolution of DIN export.

Acknowledgements

This study was supported by the Kyoto University Global COE program “Sustainability/Survivability Science for a Resilient Society Adaptable to Extreme Weather Conditions” and the JSPS Grants-in-Aid for Scientific Research. This work was also partially supported by JSPS KAKENHI, Grants-in-Aid for Scientific Research (S)(19106008). We wish to thank Dr. Lex Bouwman for providing us with global data on N input including sewage effluents, net N input via fertilizer and manure, etc., and Mr. Leif Harum for giving us good comments about this article. The authors are grateful for their supports.

REFERENCES

Alexander, R.B., Slack, J.R., Ludtke, A.S., Fitzgerald, K.K., Schertz, T.L., 1996. Data from Selected U.S. Geological Survey National Stream Water Quality Monitoring Networks (WQN) [CD-ROM]. U.S. Geol. Surv., Denver, Colo.

Baker, A., 2003. Land use and water quality. Hydrological Processes 17, 2499–2501.

Bengtsson, M., Shen, Y.J., Oki, T., 2006. A SRES-based gridded global population dataset for 1990–2100. Population and Environment 28, 113–131.

Beven, K.J., Kirkby, M.J., 1979. A physically based, variable contributing area model of basin hydrology. Hydrological Sciences Bulletin 24, 43–69.

Brisson, N., Gary, C., Justes, E., Mary, B., Roche, R., Ripoche, D., Zimmer, D., Sierra, J., Bertuzzi, P., Burger, P., Bussière, F., Cabidoche, Y.M., Cellier, P., Debaeke, P., Gaudillère, J.P., Maraux, F., Seguin, F.B., Sinoquet, H., 2003. An overview of the crop model STICS. European Journal of Agronomy 18, 309–332.

Billen, G., Garnier, J., Ficht, A., Cun, C., 1999. Nitrogen transfers through the Seine drainage network: a budget based on the application of the Riverstrahler model. Hydrobiologia 410, 139–150.

Bouwman, A.F., Lee, D.S., Asman, W.A.H., Dentener, F.J., Van Der Hoek, K.W., Oliver, J.G.J., 1997. A global high-resolution emission inventory for ammonia. Global Biogeochemical Cycles 11, 561–587.

Bouwman, A.F., Van Drecht, G., Knoop, J.M., Beusen, A.H.W., Meinardi, C.R., 2005a. Exploring changes in river nitrogen export to the world's oceans. Global Biogeochemical Cycles 19 (GB1002). doi:10.1029/2004GB002314.

Bouwman, A.F., Van Drecht, G., Van der Hoek, K.W., 2005b. Nitrogen surface balances in intensive agricultural production systems in different world regions for the period 1970–2030. Pedosphere 15 (2), 137–155.

Davis, J.R., Koop, K., 2006. Eutrophication in Australian rivers, reservoirs and estuaries – a southern hemisphere perspective on the science and its implications. Hydrobiologia 559, 23–76.

Dickinson, R.E., Shaikh, M., Bryant, R., Graumlich, L., 1998. Interactive canopies for a climate model. Journal of Climate 11, 2823–2836.

Ding, C., Ohmori, H., Takamura, H., 2006. Relationship between water quality and land use in the Mamagawa river, Tokyo Metropolitan Area. Journal of Japanese Association of Hydrological Sciences 36 (4), 219–233.

Dirmeyer, P.A., Gao, X.A., Zhao, M., Guo, Z.C., Oki, T., Hanasaki, N., 2006. GSWP-2: multimodel analysis and implications for our perception of the land surface. Bulletin of the American Meteorological Society 87, 1381–1397.

Dumont, E., Harrison, J.A., Kroeze, C., Bakker, E.J., Seitzinger, S.P., 2005. Global distribution and sources of dissolved organic nitrogen export to the coastal zone: results from a spatial explicit, global model. Global Biochemical Cycle 19 (GB4S402), 1–13.

Edwards, M.H. 1986. Digital image processing of local and global bathymetric data. M.S. thesis, Department of Earth and Planetary Sciences, Washington University, St. Louis, MO, 106pp.

Europe's Environment: Statistical Compendium for the Second Assessment, Report, 1998. European Environment Agency, Copenhagen.

FAOSTAT. http://faostat.fao.org/site/291/default.aspx.

Galloway, J.N., Schlesinger, W.H., Levy II, H., Michaels, A., Schnoor, J.L., 1995. Nitrogen fixation: anthropogenic enhancement – environmental response. Global Biogeochemical Cycles 9, 235–252.

Galloway, J.N., 1998. The global nitrogen cycle: changes and consequences. Environmental Pollution 102, 15–26.

Galloway, J.N., 2000. Nitrogen mobilization in Asia. Nutrient Cycling in Agroecosystems 57, 1–12.

Galloway, J.N., Cowling, E.B., 2002. Nitrogen and the world. Ambio 31, 64–71.

Galloway, J.N., Dentener, F.J., Capone, D.G., Boyer, E.W., Howarth, R.W., Seitzinger, S.P., Asner, G.P., Cleveland, C.C., Green, P.A., Holland, E.A., Karl, D.M., Michaels, A.F., Porter, J.H., Townsend, A.R., Vorosmarty, C.J., 2004. Nitrogen cycle: past, present and future. Biogeochemistry 70, 153–226.

Harmel, R.D., Cooper, R.J., Slade, R.M., Haney, R.L., Arnold, J.G., 2006. Cumulative uncertainty in measured streamflow and water quality data for small watersheds. Transactions of the American Society of Agricultural and Biological Engineers (ASAE) 49 (3), 689–701.

Harrison, J.A., Caraco, N., Seitzinger, S.P., 2005. Global patterns and sources of dissolved organic matter export to the coastal zone: results from a spatial explicit, global model. Global Biogeochemical Cycles 19 (GB4S04), 1–16.

Hanasaki, N., Kanae, S., Oki, T., Masuda, K., Motoya, K., Shirakawa, N., Shen, Y., Tanaka, K., 2008. An integrated model for the assessment of global water resources—Part 2: applications and assessment. Hydrology and Earth System Sciences 12, 1027–1037.

Hantschel, R.E., Beese, F., 1997. Site-oriented ecosystem management: precondition to reducing the contamination of waters and the atmosphere. In: Rosen, D., Tel-Or, E., Hadar, Y., Chen, Y. (Eds.), Modern Agriculture and the Environment. Kluwer Academic Publishers, Dordrecht, pp. 135–145.

He, B., Oki, T., Kanae, S., Mouri, G., Kodama, K., Komori, D., Seto, S., 2009a. Integrated biogeochemical modelling of nitrogen load from anthropogenic and natural sources in Japan. Ecological Modelling 220, 2325–2334.

He, B., Oki, K., Wang, Y., Oki, T., 2009b. Using remotely sensed imagery to estimate potential annual pollutant loads in river basins. Water Science and Technology 60 (8), 2009–2015. doi: 10.2166/wst.2009.596.

Hirabayashi, Y., Kanae, S., Oki, T., 2005. A 100-year (1901–2000) global retrospective estimation of terrestrial water cycle. Journal of Geophysical Research 110, D19101.

Hirabayashi, Y., Kanae, S., Emori, S., Oki, T., Kimoto, M., 2008. Global projections of changing risks of floods and droughts in a changing climate. Hydrological Sciences Journal 53 (4), 754–772.

Howarth, R.W., Sharpley, A., Walker, D., 2002. Sources of nutrient pollution to coastal waters in the United States: implications for achieving coastal water quality goals. Estuaries 25 (4B), 656–676.

Hudson, D., Hite, D., Haab, T., 2005. Public perception of agricultural pollution and Gulf of Mexico hypoxia. Coastal Management 33 (1), 25–36.

Hudson, R.J.M., Gherini, S.A., Goldstein, R.A., 1994. Modelling the global carbon cycle: nitrogen fertilization of the terrestrial biosphere and the 'missing' CO_2 sink. Global Biogeochemical Cycles 8 (3), 307–333.

Jacks, G., Sharma, V.P., 1983. Nitrogen circulation and nitrate in groundwater in an agricultural catchment in southern India. Environment Geology 5, 61–64.

Johnsson, H., Bergström, L., Jansson, P.E., Paustian, K., 1987. Simulated nitrogen dynamics and losses in a layered agricultural soil. Agriculture Ecosystems and Environment 18 (4), 333–356.

Lewis, J.R.W.M., Melack, J.M., McDowell, W.H., McClain, M., Richey, J.E., 1999. Nitrogen yields from undisturbed watersheds in the America. Biogeochemistry 46, 149–162.

Lin, B.L., Sakoda, A., Shibasaki, R., Goto, N., Suzuki, M., 2000. Modelling a global biogeochemical nitrogen cycle model in terrestrial ecosystems. Ecological Modelling 135-1, 89–110.

Lin, B.L., Sakoda, A., Shibasaki, R., Suzuki, M., 2001. A modelling approach to global nitrate leaching caused by anthropogenic fertilisation. Water Research 35 (8), 1961–1968.

Loveland, T.R., Reed, B.C., Brown, J.F., Ohlen, D.O., Zhu, J., Yang, L., Merchant, J.W., 2000. Development of a global land cover characteristics database and IGBP DISCover from 1-km AVHRR data. International Journal of Remote Sensing 21 (6/7), 1,303–1,330.

Manabe, S., Stouffer, R.J., Spelman, M.J., Bryan, K., 1991. Transient responses of a coupled ocean-atmosphere model to gradual changes of atmospheric CO_2. Part I: annual mean response. Journal of Climate 4, 785–818.

Manabe, S., Spelman, M.J., Stouffer, R.J., 1992. Transient responses of a coupled ocean-atmosphere model to gradual changes of atmospheric CO_2. Part II: seasonal response. Journal of Climate 5, 105–126.

Ngo-Duc, T., Oki, T., Kanae, S., 2007. A variable stream flow velocity method for global river routing model: model description and preliminary results. Hydrology and Earth System Sciences Discussions 4, 4389–4414.

Oenema, O., Boers, P.C.M., Willems, W.J., 1998. Leaching of nitrate from agriculture to groundwater: the effect of policies and measures in the Netherlands. Environmental Pollution 102, 471–478.

Oki, T., Nishimura, T., Dirmeyer, P., 1999. Assessment of annual runoff from land surface models using Total Runoff Integrating Pathways (TRIP). Journal of the Meteorological Society of Japan 77 (1B), 235–255.

Oki, T., Sud, Y.C., 1998. Design of total runoff integrating Pathways (TRIP) – A global river channel network. Earth Interactions 2.

Rijtema, P.E., Kroes, J.G., 1991. Some results of nitrogen simulations with the model ANIMO. Fertilizer Research 27, 189–198.

Sakamoto, T.T., Emori, S., Nishimura, T., Hasumi, H., Suzuki, T., Komoto, M., 2004. Far-reaching effects of the Hawaiian Islands in the CCSR/NIES/FRCGC high-resolution climate model. Geophysical Research Letters 31, L17212.

Sakimura, T., 2007. Development of an approach to predict flood risks based on water and energy balance simulation over Japan. Master Thesis. The University of Tokyo.

Schepers, J.S., Varvel, G.E., Watts, D.G., 1995. Nitrogen and water management strategies to reduce nitrate leaching under irrigated maize. Journal of Contaminant Hydrology 20, 227–239.

Seitzinger, S.P., 1995. Data Collection Program in Support of the Harborwide Eutrophication Model for New York – New Jersey Harbor Estuary Program, Report. U.S. Environ. Prot. Agency, New York.

Seitzinger, S.P., Kroeze, C., 1998. Global distribution of nitrous oxide production and N inputs in freshwater and coastal marine ecosystems. Global Biochemical Cycles 12, 93–113.

Seitzinger, S.P., Harrison, J.A., Dumont, E., Beusen, A.H.W., Bouwman, A.F., 2005. Sources and delivery of carbon, nitrogen, and phosphorus to the coastal zone: an overview of global Nutrient Export from Watersheds (NEWS) models and their application. Global Biogeochemical Cycles 19 (GB4S01), 1–11.

Sellers, P.J., Randall, D.A., Collatz, G.J., Berry, J.A., Field, C.B., Dazlich, D.A., Zhang, C., Collelo, G.D., Bounoua, L., 1996. A revised land surface parameterization (SiB2) for atmospheric GCMs. Part I: model formulation. Journal of Climate 9, 676–705.

Sferratore, A., Billen, G., Garnier, J., Thery, S., 2005. Modeling nutrient budget in the Seine watershed: application of the Riverstrachler model using data from local to global scale resolution. Global Biogeochemical Cycles 19, 1–14. doi:10.1029/2005GB002496.

Shaffer, M.J., Halvorson, A.D., Pierce, F.J., 1991. Nitrate leaching and economic analysis package (NLEAP): model description and application. In: Follet, R.F., Keeney, D.R., Cruse, R.M. (Eds.), Managing Nitrogen for Groundwater Quality and Farm Profitability. Soil Science Society of America, Madison, Wis, pp. 285–322.

Shindo, J., Okamoto, K., Kawashima, H., 2003. A model-based estimation of nitrogen flow in the food production – supply system and its environmental effects in East Asia. Ecological Modeling 169, 197–212.

Shindo, J., Okamoto, K., Kawashima, H., 2006. Prediction of the environmental effects of excess nitrogen caused by increasing food demand with rapid economic growth in eastern Asian countries, 1961–2020. Ecological Modelling 193 (3–4), 703–720.

Stouffer, R.J., Manabe, S., Vinnikov, K.Y., 1994. Model assessment of the role of natural variability in recent global warming. Nature 367, 634–636.

Subramanian, V., 2004. Water quality in South Asia. Asian Journal of Water, Environment and Pollution 1, 41–54.

Takata, K., 2000. Sensitivity Study on Snowmelt Discharge of Lena Using a Land Surface Model, "MATSIRO". Activity Report of GAME-Siberia, 1999. No. 21, Nagoya Univ.. GAME Publication, Nagoya, Japan, pp. 73–76.

Takata, K., 2001. Estimation of Summer Heat and Water Fluxes at Tiksi Using a One-dimensional Land Surface Model. Activity Report of GAME-Siberia, 2000. No. 26, Nagoya Univ.. GAME Publication, Nagoya, Japan, pp. 207–208.

Takata, K., Emori, S., Watanabe, T., 2003. Development of the minimal advanced treatments of surface interaction and runoff. Global and Planetary Change 38, 209–222.

Thornton, P.E., Rosenbloom, N.A., 2005. Ecosystem model spin-up: estimating steady state conditions in a coupled terrestrial carbon and nitrogen cycle model. Ecological Modelling 189, 25–48.

United Nations, 1996. Country Population Statistics and Projections 1950–2050, Report. Food and Agric. of the U.N., Rome.

USGS. http://edc2.usgs.gov/glcc/globdoc2_0.php.

Van Drecht, G., Bouwman, A.F., Knoop, J.M., Beusen, A.H.W., Meinardi, C.R., 2003. Global modeling of the fate of nitrogen from point and nonpoint sources in soils, groundwater, and surface water. Global Biogeochemical Cycles 17 (4), 1–20. doi: 10.1029/2003GB002060.

Veuger, B., Middelburg, J.J., Boschker, H.T.S., Nieuwenhuize, J., van Rijswijk, P., Rochelle-Newall, E.J., Navarro, N., 2004. Microbial uptake of dissolved organic and inorganic nitrogen in Randers Fjord. Estuarine Coastal and Shelf Science 61, 507–515.